

Copyright WILEY-VCH Verlag GmbH & Co. KGaA, 69469 Weinheim, Germany, 2018.

Supporting Information

Oxidation-responsive, tunable growth factor delivery from polyelectrolyte-coated implants

*John R. Martin, MayLin T. Howard, Sheryl Wang, Adam G. Berger, Paula T. Hammond**

SI Methods

Thioketal Monomer and PTK-BAA Polymer: Synthesis and Characterization: Adapted from previously reported methods^[34a], cysteamine hydrochloride (8.0 g, 70 mmol, 1.0 equiv) was first dissolved in 100 mL methanol with triethylamine (10.6 g, 105 mmol, 1.5 equiv) before adding ethyl trifluoroacetate (11.9 g, 84 mmol, 1.2 equiv) and mixing overnight. The trifluoroacetate-protected cysteamine was extracted from the generated salt byproduct with 2x ethyl acetate washes and dried under rotary evaporation. To ensure free thiols are present for thioketal synthesis, the protected cysteamine (8.7 g, 50 mmol, 1.0 equiv) was dissolved in 100 mL anhydrous methanol along with the reducing agent tris(2-carboxyethyl) phosphine hydrochloride (TCEP HCl, 3.1 g, 12.5 mmol, 0.25 equiv) and mixed under nitrogen for 4h. Next, methanol was removed by rotary evaporation and the reduced product was extracted with 3x washes of anhydrous dichloromethane (antisolvent for TCEP). Thiol presence was confirmed with the Ellman's assay according to manufacturer's protocols, and structure was confirmed by ¹H NMR (Bruker Avance-III HD Nanobay spectrometer, 400 MHz, CDCl₃): δ 1.42 (1H, CF₃CONHCH₂CH₂SH); δ 2.75 (2H, CF₃CONHCH₂CH₂SH); δ 3.56 (2H, CF₃CONHCH₂CH₂SH); δ 6.85 (1H, CF₃CONHCH₂CH₂SH).

To synthesize the protected thioketal diamine monomer, the reduced trifluoroacetate-cysteamine (7.8 g, 45 mmol, 1.0 equiv) was dissolved in anhydrous acetonitrile with the

catalyst *p*-toluenesulfonic acid monohydrate (0.34 g, 1.8 mmol, 0.04 equiv). Next, 2,2 dimethoxypropane (4.7 g, 45 mmol, 1.0 equiv) was added and mixed overnight under positive nitrogen pressure for 16h. The crude protected thioketal diamine was dried by rotary evaporation and then dissolved in 50 mL of aqueous 6 M NaOH to cleave the trifluoroacetate groups. After mixing for 4h, the thioketal diamine product was extracted with 3x washes with dichloromethane and dried. ^1H NMR (400MHz, CDCl_3):

δ 1.54 (4H, $\text{NH}_2\text{CH}_2\text{CH}_2\text{SC}(\text{CH}_3)_2\text{SCH}_2\text{CH}_2\text{NH}_2$);

δ 1.62 (6H, $\text{NH}_2\text{CH}_2\text{CH}_2\text{SC}(\text{CH}_3)_2\text{SCH}_2\text{CH}_2\text{NH}_2$);

δ 2.75 (4H, $\text{NH}_2\text{CH}_2\text{CH}_2\text{SC}(\text{CH}_3)_2\text{SCH}_2\text{CH}_2\text{NH}_2$);

δ 2.93 (4H, $\text{NH}_2\text{CH}_2\text{CH}_2\text{SC}(\text{CH}_3)_2\text{SCH}_2\text{CH}_2\text{NH}_2$);

To synthesize the thioketal diacrylamide monomer, thioketal diamine (2.6 g, 13.5 mmol, 1.0 equiv) was dissolved in 100 mL of tetrahydrofuran (THF) with triethylamine (6.8 g, 67.5 mmol, 5.0 equiv) on ice. Next, acryloyl chloride (4.9 g, 54 mmol, 4.0 equiv) was added drop-wise to the solution under constant stirring before letting react overnight. THF was then removed by rotary evaporation before removing the crude product from the salt byproduct with 2x ethyl acetate rinses. Next, the purified compound was extracted by silica gel chromatography using a 1:3 v/v ratio of ethyl acetate to hexane before drying. ^1H NMR (400MHz, CDCl_3):

δ 1.61 (6H, $\text{CH}_2\text{CHCONHCH}_2\text{CH}_2\text{SC}(\text{CH}_3)_2\text{SCH}_2\text{CH}_2\text{NHCOCHCH}_2$);

δ 2.85 (4H, $\text{CH}_2\text{CHCONHCH}_2\text{CH}_2\text{SC}(\text{CH}_3)_2\text{SCH}_2\text{CH}_2\text{NHCOCHCH}_2$);

δ 2.85 (4H, $\text{CH}_2\text{CHCONHCH}_2\text{CH}_2\text{SC}(\text{CH}_3)_2\text{SCH}_2\text{CH}_2\text{NHCOCHCH}_2$);

δ 3.57 (4H, $\text{CH}_2\text{CHCONHCH}_2\text{CH}_2\text{SC}(\text{CH}_3)_2\text{SCH}_2\text{CH}_2\text{NHCOCHCH}_2$);

δ 5.66 (2H, $\text{CH}'\text{H}''\text{CHCONHCH}_2\text{CH}_2\text{SC}(\text{CH}_3)_2\text{SCH}_2\text{CH}_2\text{NHCOCHCH}'\text{H}''$);

δ 6.16 (2H, $\text{CH}_2\text{CHCONHCH}_2\text{CH}_2\text{SC}(\text{CH}_3)_2\text{SCH}_2\text{CH}_2\text{NHCOCHCH}_2$);

δ 6.23 (4H, $\text{CH}_2\text{CHCONHCH}_2\text{CH}_2\text{SC}(\text{CH}_3)_2\text{SCH}_2\text{CH}_2\text{NHCOCHCH}_2$);

δ 6.31 (4H, $\text{CH}'\text{H}''\text{CHCONHCH}_2\text{CH}_2\text{SC}(\text{CH}_3)_2\text{SCH}_2\text{CH}_2\text{NHCOCHCH}'\text{H}''$);

To prevent self-polymerization of the acrylamide end-groups, the thioketal diacrylamide (0.85 g, 2.8 mmol, 1.0 equiv) was then immediately taken and dissolved in 30 mL of a 3:1 v/v mix of ethanol:water along with 4,4'-trimethylene dipiperidine (0.6 g, 2.86 mmol, 1.02 equiv) for 24h at room temperature under positive nitrogen pressure. Longer polymerization times (i.e. 7 days) or higher temperatures were not shown to increase molecular weight, and the use of an ethanol/water polymerization solvent was chosen based on literature precedent^[36] and poor polymerization efficiencies achieved with previously reported THF^[52] or DMF^[34a]. The resultant PTK-BAA polymer was dried under rotary evaporation, and then precipitated 3x into cold THF to separate the insoluble polymer from the THF-soluble monomers. Polymer molecular weight was characterized by MALDI-TOF using a Bruker Autoflex LRF Speed mass spectrometer in linear mode with 2,5-dihydroxybenzoic acid (DHB) as the matrix. Samples were prepared by mixing 10 mg mL⁻¹ DHB with 1 mg mL⁻¹ PTK-BAA (both dissolved in methanol) before adding 1 μ L of mixed solution to the detector target, drying, and collecting spectral data. ¹H NMR (400MHz, CDCl₃):

δ 1.17-1.35 (12H, -N(CH'H''CH'H'')₂CH(CH₂)₃CH(CH''H'CH'' H')₂N-)

δ 1.61 (6H, -NCH₂CH₂CONHCH₂CH₂SC(CH₃)₂SCH₂CH₂NHCOCH₂CH₂N-)

δ 1.72 (4H, -N(CH'H''CH'H'')₂CH(CH₂)₃CH(CH'' H'CH'' H')₂N-)

δ 1.96 (4H, -N(CH'H''CH'H'')₂CH(CH₂)₃CH(CH'' H'CH'' H')₂N-)

δ 2.38 (4H, -NCH₂CH₂CONHCH₂CH₂SC(CH₃)₂SCH₂CH₂NHCOCH₂CH₂N-)

δ 2.58 (4H, -N(CH'H''CH'H'')₂CH(CH₂)₃CH(CH'' H'CH'' H')₂N-)

δ 2.76 (4H, -NCH₂CH₂CONHCH₂CH₂SC(CH₃)₂SCH₂CH₂NHCOCH₂CH₂N-)

δ 2.96 (4H, -NCH₂CH₂CONHCH₂CH₂SC(CH₃)₂SCH₂CH₂NHCOCH₂CH₂N-)

δ 3.46 (4H, -NCH₂CH₂CONHCH₂CH₂SC(CH₃)₂SCH₂CH₂NHCOCH₂CH₂N-)

PBAE Synthesis and Characterization: Adapted from previously established protocols^[19b, 52], a poly(β -amino ester) (PBAE) polycation was synthesized via Michael addition condensation polymerization. 1,6 hexanediol diacrylate (6.65 g, 29.5 mmol, 1.0 equiv) was dissolved in 20 mL of anhydrous THF, while 4,4'-trimethylene dipiperidine (6.31 g, 30 mmol, 1.02 equiv) was dissolved in a separate aliquot of anhydrous THF and then added to the diacrylate solution. The reaction was allowed to proceed for 48h under nitrogen at 50°C. The crude PBAE product was purified by 3x precipitations into -20°C diethyl ether/hexane (1:1 v/v ratio) and then dried. The polymer's molecular weight was determined via gel permeation chromatography (GPC) using a Waters system with Styragel columns (Milford, MA), THF mobile phase, and linear polystyrene molecular weight standards. ¹H NMR (400MHz, CDCl₃):

δ 1.14-1.35 (12H, -N(CH'H"CH'H")₂CH(CH₂)₃CH(CH'H'CH" H')₂N-)

δ 1.38 (4H, -NCH₂CH₂COOCH₂CH₂CH₂CH₂CH₂CH₂OCOCH₂CH₂N-)

δ 1.56 (4H, -NCH₂CH₂COOCH₂CH₂CH₂CH₂CH₂CH₂OCOCH₂CH₂N-)

δ 1.65 (4H, -N(CH'H"CH'H")₂CH(CH₂)₃CH(CH'H'CH" H')₂N-)

δ 1.96 (4H, -N(CH'H'CH'H")₂CH(CH₂)₃CH(CH" H'CH" H')₂N-)

δ 2.50 (4H, -NCH₂CH₂COOCH₂CH₂CH₂CH₂CH₂CH₂OCOCH₂CH₂N-)

δ 2.66 (4H, -N(CH'H"CH'H")₂CH(CH₂)₃CH(CH" H'CH" H')₂N-)

δ 2.86 (4H, -NCH₂CH₂COOCH₂CH₂CH₂CH₂CH₂CH₂OCOCH₂CH₂N-)

δ 4.06 (4H, -NCH₂CH₂COOCH₂CH₂CH₂CH₂CH₂CH₂OCOCH₂CH₂N-)

Hexane-PBAA Synthesis and Characterization: Following the protocol for PTK-BAA synthesis, 1,6 hexanediamine (1.51 g, 13 mmol, 1.0 equiv) was dissolved in THF alongside triethylamine (3.95 g, 39 mmol, 3.0 equiv). While mixing the solution on ice, acryloyl chloride (3.53 g, 39 mmol, 3.0 equiv) was slowly added and allowed to stir overnight. THF was removed by rotary evaporation before separating the crude product from the salt

byproduct with 2x ethyl acetate rinses, and the final product was purified by silica gel chromatography using a 1:3 v/v ratio of ethyl acetate to hexane before drying. To prevent self-polymerization of the acrylamide end-groups, the hexane diacrylamide (0.373 g, 1.67 mmol, 1.0 equiv) was then immediately taken and dissolved in 20 mL of a 3:1 v/v mix of ethanol:water along with 4,4'-trimethylene dipiperidine (0.358 g, 1.7 mmol, 1.02 equiv) for 24h at room temperature under positive nitrogen pressure. The resultant hexane-poly(β -amino amide) (hexane-PBAA) polymer was dried under rotary evaporation, and then precipitated 3x into cold THF to separate the insoluble polymer from the THF-soluble monomers. The purified polymer was then characterized by ^1H NMR in deuterated water with 0.1% trifluoroacetic acid to aid solubility.

LbL Film Construction and In Vitro Drug Release with the Model Protein Lysozyme: The low-cost model protein lysozyme was first labeled with fluorescein isothiocyanate (FITC) to allow for simple protein quantification. Lysozyme was dissolved at 5 mg mL⁻¹ in 0.1 M sodium carbonate buffer (pH 9) before slowly adding FITC dissolved in DMSO at 1 mg mL⁻¹ and stirring in the dark for 4h at 4°C. The molar feed ratio of lysozyme to FITC was 4:1. Following mixing, the FITC-labeled protein was dialyzed against deionized water using 6-8 kDa molecular weight cutoff dialysis tubing for 48h and with multiple solvent changes to remove unconjugated fluorophore. The purified FITC-lysozyme solution was then lyophilized and stored as a dried powder at 4°C.

To prepare dipping solutions for LbL film construction, all components were dissolved in 100mM sodium acetate buffer (pH 5.0). PTK-BAA was prepared at 0.5 mg mL⁻¹, poly(acrylic acid) (PAA, $M_v = 450$ kDa) at 1 mg mL⁻¹, and lysozyme at 1 mg mL⁻¹ (10% of dry mass protein with FITC-labeling). To conserve solution volume and constituent stocks, solutions were made at 5 mL volumes and placed in multichannel pipette reservoirs. For forming the LbL films, model silicon substrates (individual dimensions ~ 0.5 cm x 2 cm) were

first cleaned with ethanol and then water before drying under vacuum. The substrates were then attached to a dipper harness and plasma etched in oxygen at high RF power for 5 min using a Harrick PDC-32G plasma cleaner. Immediately following plasma cleaning, the substrates were immersed in the PTK-BAA solution (first deposition in the LbL cycle) for 15 min prior to beginning the full dipping cycle. Running at room temperature, the dipping cycles were controlled and administered with a Carl Zeiss HMS Series Programmable Slide Stainer to form cyclic depositions of tetralayer units on the silicon substrates. Tetralayers were composed of alternatively dipped 1) degradable polycation PTK-BAA, 2) polyanion PAA, 3) cationic lysozyme, and 4) PAA; each dip step was administered for 5 min, followed by two 30s washes in deionized water. PTK-BAA / lysozyme LbL films were fabricated with 30 tetralayers, and after deposition the films were allowed to dry before usage. To measure lysozyme release from the LbL films, coated silicon substrates were incubated at 37°C in 1 mL of either PBS, PBS with 0.1 mM H₂O₂, or PBS with 1 mM H₂O₂. At pre-determined time points (at least every 3-5 days to prevent peroxide decomposition and loss of oxidative potential), the coated samples were removed and placed in fresh treatment media, while the lysozyme releaseate was quantified for fluorescein fluorescence at 490 nm / 525 nm excitation/emission wavelengths using a Tecan microplate reader and normalized to a FITC-lysozyme calibration curve.

LbL Film Construction and Characterization with BMP-2: To allow for PEM film visualization and drug loading quantification, BMP-2 was first labeled with fluorescent Cy5 or Cy7-NHS ester. BMP-2 was dissolved in 50 mM sodium carbonate buffer (adjusted to pH 7) at 3 mg mL⁻¹ before adding a 20x molar excess of Cy5-NHS ester dissolved at 10 mg mL⁻¹ in dimethylsulfoxide and mixing for 3h at 4°C. Though BMP-2 is less soluble at pH 7, this neutral pH was chosen to ensure sufficient conjugation between the protein's free amine groups and the dye's NHS ester as this reaction proceeds most favorably under basic

conditions. After the reaction was completed, the labeled protein solution was diluted into the same sodium carbonate buffer and spun at $4000 \times g$ for 25 min through a 3 kDa molecular weight cutoff spin filter (Amicon) to remove unreacted dye, and following the initial spin the retained protein solution was diluted again and re-spun two more times. The final dye-labeled BMP-2 concentration was quantified by ELISA and stocks were stored at -80°C for further usage. Film construction with BMP-2 was carried out similarly to the methods described above for lysozyme films. Deposition solutions of the initial polycation (PTK-BAA, PBAE, or hexane-PBAA) were prepared at 0.5 mg mL^{-1} in 100 mM sodium acetate buffer at pH 5.0. Solutions for 450, 5, or 1.8 kDa molecular weight PAA were created at 1 mg mL^{-1} in the same pH 5.0 buffer. BMP-2 was dissolved at $40 \mu\text{g mL}^{-1}$ in 100 mM sodium acetate buffer adjusted to pH 4.1, and solutions with Cy5-BMP-2 were doped with 5% by mass labeled protein alongside 95% unlabeled BMP-2. LbL films were formed on plasma-cleaned silicon substrates (5 min treatment) or PLGA scaffolds (15s treatment), and following plasma cleaning the substrates were submersed in the first polycation solution for 30 min before progressing into the dipping cycles. Tetralayer units were composed of 1) degradable polycation (5 min dip), 2) PAA (5 min dip), 3) BMP-2 (10 min dip), and 4) PAA (5 min dip) with $2 \times 30\text{s}$ rinses in deionized water between dips, and these cycles were repeated until the final number of tetralayer depositions was reached. Both the top and bottom surfaces of the substrates were coated.

LbL film thickness as a function of tetralayer depositions for PTK-BAA / BMP-2 films fabricated with 450 kDa PAA on flat silicon substrates was evaluated using a Dektak Stylus profilometer (Veeco Instruments Inc.). Dry films were scratched with a razor blade to expose the underlying silicon, and then the perpendicular distance between the silicon and the film surface (i.e. film thickness) was measured at the distal, proximal, and medial sections on the silicon. To quantify BMP-2 loading vs. number of tetralayers, PTK-BAA / Cy5-BMP-2 films constructed with 450 kDa PAA on PLGA scaffolds were first punched out using a

biopsy punch, fluorescently imaged with an IVIS Spectrum (Perkin Elmer) using 640 nm / 680 nm excitation/emission filters with 0.75s exposure time, and analyzed for total radiant efficiency per 8 mm diameter scaffold ($\sim 1 \text{ cm}^2$ total film area on scaffold surfaces). These same scaffold samples were then incubated for 48h in 1 mL PBS doped with 10 mM H_2O_2 at 37°C to fully degrade the PTK-BAA films, and this releaseate was analyzed by ELISA to quantify total BMP-2.

In Vitro BMP-2 Release from LbL Films: LbL films comprising BMP-2, 450 kDa PAA, and either PTK-BAA or PBAE degradable polycations were deposited on PLGA scaffolds with 30 tetralayer repeats. After drying, the coated PLGA samples were cut into $\sim 0.4 \text{ cm} \times 1 \text{ cm}$ pieces and incubated at 37°C in 1 mL of either PBS or PBS with 1 mM H_2O_2 . At pre-determined timepoints, the film-coated PLGA samples were transferred into fresh 1 mL aliquots of treatment media and the releaseate samples were frozen at -20°C before measuring BMP-2 concentrations using ELISA. For this study, the cumulative BMP-2 release at day 15 from H_2O_2 -treated films was designated as 100% release due to the plateaued kinetics.

For measuring responsive BMP-2 release from these fabricated PTK-BAA films, coated PLGA samples were initially incubated in either 1 mL PBS or PBS with 1 mM H_2O_2 at 37°C. Samples were transferred to fresh aliquots of the same treatment media at days 1 and 3 and releaseate was collected. At day 4, the peroxide-treated samples were transferred to fresh H_2O_2 media and treated with this ROS-doped solution for the duration of the experiment. Alternatively, the previously PBS-incubated samples were transferred instead to 1 mM H_2O_2 treatment media and incubated in ROS-doped media for 4 days. After this period of ROS treatment, the PBS-to- H_2O_2 samples were switched again to PBS media for 4 days; this 4-day back and forth treatment pulsing was continued until day 20. For both the “constant” and “pulsed” ROS-treated samples, releaseate was collected every two days and then quantified for BMP-2 amounts (normalized to scaffold areas) by ELISA.

To determine the effects of PAA molecular weight on protein release from LbL films, PTK-BAA / Cy5-BMP-2 films were fabricated with 450, 5, and 1.8 kDa PAA with 30 tetralayer repeats on PLGA substrates. The coated PLGA scaffolds were first fluorescently imaged by IVIS to visualize and quantify relative BMP-2 loading. Next, the film-coated scaffolds were incubated at 37°C in 1 mL of either PBS, PBS with 0.1 mM H₂O₂, or PBS with 1 mM H₂O₂; samples were transferred every 3-4 days into fresh treatment media, and releaseate was collected and stored at -20°C before quantifying BMP-2 concentrations (normalized to scaffold areas) using ELISA. Control LbL films were also constructed with Cy5 BMP-2, 1.8 kDa PAA, and either the hydrolytically-sensitive PBAE or non-degradable hexane-PBAA polycations on PLGA substrates with 30 tetralayer repeats. Release experiments and quantifications were performed with the same methodologies as used for PTK-BAA film samples.

In Vitro Osteogenic Bioactivity of Film-Released BMP-2: MC3T3-E1 cells were seeded into a 24-well plate at 5.0×10^4 cells per well in 1 mL of culture media. Releaseate samples from 30 tetralayer PTK-BAA / 450 kDa PAA / BMP-2 films incubated in either PBS or PBS with 1 mM H₂O₂ were pooled to create 5 distinct subsets: day 1, days 2-5, days 6-12, days 13-19, and days 20-22. Additional PBS was added to samples as needed to give each subset the same volume. Using ELISA quantitation of BMP-2 concentrations from the day 1 pool, an identical volume aliquot (enough to give a 25 ng mL⁻¹ dose of BMP-2 from the day 1 pool) was taken from each pooled sample and lyophilized for 48h to concentrate and remove residual cytotoxic H₂O₂. Freeze-dried samples were reconstituted into fresh media and administered to the plated MC3T3-E1 cells for 48h before changing treatment to pro-differentiation media (standard media with additional 50 µg mL⁻¹ ascorbic acid and 10 mM β-glycerophosphate) and continuing culture for an additional 4 days. Alkaline phosphatase (ALP) activity was quantified after day 6 using p-nitrophenyl phosphate (pNPP) as the enzyme substrate, and the

assay was performed following manufacturer instructions. Briefly, treated cells were washed with cold PBS and collected by centrifugation at 1000 rpm for 5 minutes. Cells were re-suspended in 400 μ L Assay Buffer to lyse cells followed by centrifugation at 14000 rpm at 4°C for 15min. To perform the ALP assay, 80 μ L of each sample supernatant was transferred in triplicate to a 96-well plate and 50 μ L of pNPP solution was added to each well. The plate was mixed and incubated at 25°C for 60 min protected from light before adding 20 μ L stop solution to each well and then recording absorbance at 405 nm using a microplate reader. Sample absorbance readings were compared to a standard curve generated using reconstituted ALP enzyme to obtain ALP activity and normalized to total protein content in cell lysate as measured by the Coomassie (Bradford) protein assay.

Microcomputed Tomography Analysis: To evaluate bone regeneration at 4-weeks post-surgery and implant placement, rats were anesthetized and inserted into the bore of a GE eXplore CT 120 (GE Healthcare, Chicago, IL) system and scanned at 1° rotation angles for a total of 360 scans. The scans were collected using a 0.5mm aluminum filter, 100 kV x-ray potential, 50 mA current, gain and offset of 0, 20 ms exposure (integration) time, and 2 x 2 binning before being reconstructed at 50 μ m isotropic resolution with GPU CT Reconstruction software (Parallax Innovations). Bone volume analysis was performed in Microview (Parallax Innovations) by positioning an 8 mm-diameter cylindrical ROI in the center of the nominally 8 mm-diameter defect and measuring both mature (gray-level threshold > 1000) and immature bone (gray level threshold > 350) volumes contained in the ROI as determined with the software's Bone Analysis tool. Tissue mineral density was also determined from this same ROI using the Microview Bone Analysis tool. Volumetric reconstructions of mature and immature bone were overlaid using Adobe Photoshop.

For evaluating bone regeneration in the additional rat cohort featuring scaffold implants coated with the combination PTK₁₅/PBAE₁₅ BMP-2 films, the animals were

scanned with a Bruker Skyscan 1276 Micro-CT system due to hardware upgrades being undertaken in the Koch Institute Preclinical Imaging core facility. These animals were scanned at 0.5° rotation angles over 180° for a total of 360 scans, and were collected using an aluminum-copper filter, 100 kV x-ray potential, 200 μ A current, 468 ms exposure (integration) time, and 2 x 2 binning before being reconstructed at 20.1 μ m isotropic resolution with GPU-based NRecon software (Bruker). Bone volume analysis was performed in Microview using an 8 mm-diameter cylindrical ROI as described above, but employing a gray-level threshold value of 20,000 for selectively visualizing bone tissue and quantifying bone volumes. Due to the two different CT systems and shifted parameters used in evaluating these various animal cohorts, direct bone growth comparisons between treatment groups scanned on different machines proved difficult. To create a comparative approximation, bone growth for the different groups was normalized to expected bone volume in an 8 mm calvarial ROI as measured in healthy rats (estimated at $\sim 52 \text{ mm}^3$ for the GE system scan and $\sim 31 \text{ mm}^3$ for the Bruker system scan). The higher resolution Bruker scans were able to detect finer details of marrow and void volumes in the bone, causing the apparent decrease in measured bone tissue volume for a similarly sized ROI. Therefore, measured bone volumes within the 8 mm calvarial ROIs for film-treated animals were normalized to expected full defect volume from each respective scanner and presented as percent defect filled.

Histological Sample Preparation: Rats were euthanized at week 4 for histological analysis. Intact calvarial bone was extracted and fixed in 10% neutral-buffered formalin for 5 days before decalcifying in 10% v/v formic acid (changed every 3 days) for 1 week. Finally, the bone sample was bisected along the skull's midline sagittal suture with a sharp razor blade before submitting for histological processing. Samples were embedded in paraffin, cut into 5 μ m thick sections, and stained with hematoxylin and eosin (H&E) for visualization. Slide images were further analyzed using open-source QuPath software. For samples prepared for

immunohistochemical (IHC) staining, commercial mouse anti-rat CD68 antibodies (MCA341GA, Bio-Rad, 1:200 dilution) were used for primary incubation before secondary incubation with ImmPRESS HRP anti-mouse IgG polymer detection kit (Vector Laboratories). IHC slides were also counterstained with hematoxylin for nuclei visualization.

In Vivo IVIS Analysis: To evaluate *in vivo* BMP-2 release kinetics from ROS-sensitive PTK-BAA films as benchmarked against conventional PBAE formulations, PLGA scaffolds were coated with 30 tetralayer PEM films comprising Cy7-tagged BMP-2 (40% labeled), 1.8 kDa PAA, and either the PTK-BAA or PBAE polycation. Additional film samples featuring Cy-7 BMP-2, 1.8 kDa PAA, and “stacked” combination coatings with an inner 15 tetralayers of PTK-BAA and outer 15 tetralayers of PBAE polymers were also fabricated and evaluated *in vivo*. After surgical creation of 8.0 mm rat calvarial defects, the fluorescently-labeled samples were implanted into the respective defects as described above (n=3 animals per treatment). Following animal recovery, the rats were fluorescently imaged on day 0 with an IVIS Spectrum using 710 nm / 780 nm excitation/emission wavelengths. Imaging was subsequently performed at days 1, 2, 4, 7, 11, 14, 17, and 21 post-surgery and normalized to day 0 values to quantify BMP-2 retention over time. Half-life values were calculated from a least-squares nonlinear fit of a one-phase decay equation ($R^2 > 0.95$ goodness of fit for both curves) to the BMP-2 release data using GraphPad Prism and are displayed with the 95% confidence interval from the generated fit.

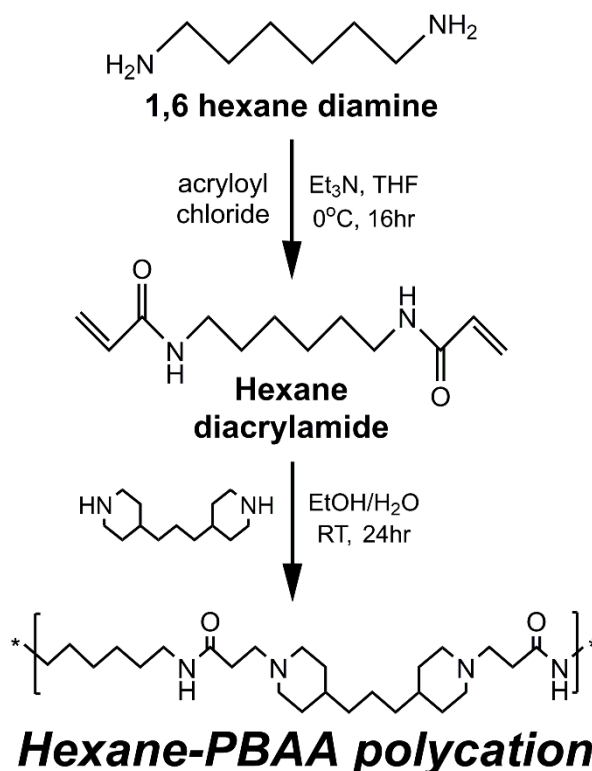


Figure S1. Synthetic scheme for the non-degradable hexane-poly(β -amino amide) polycation.

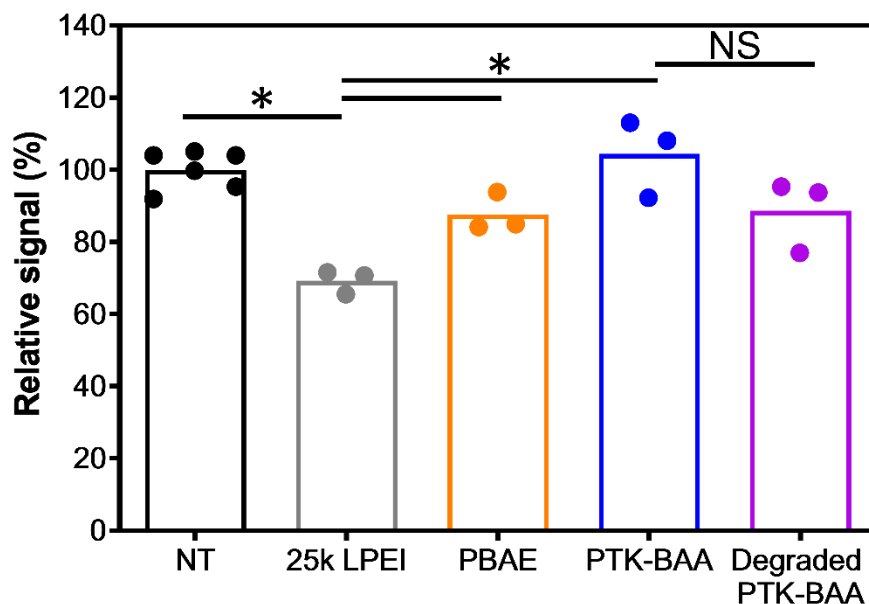


Figure S2. *In vitro* polycation toxicity. MC3T3-E1 pre-osteoblasts were incubated for 24h in media doped with $10 \mu\text{g mL}^{-1}$ of each respective polycation, with the control LPEI displaying significantly more toxicity than no treatment (NT), PBAE, or PTK-BAA incubation (* $p < 0.05$). Moreover, PTK-BAA degradation products generated after treatment with 10 mM H₂O₂ were not significantly more cytotoxic than the parent polymer

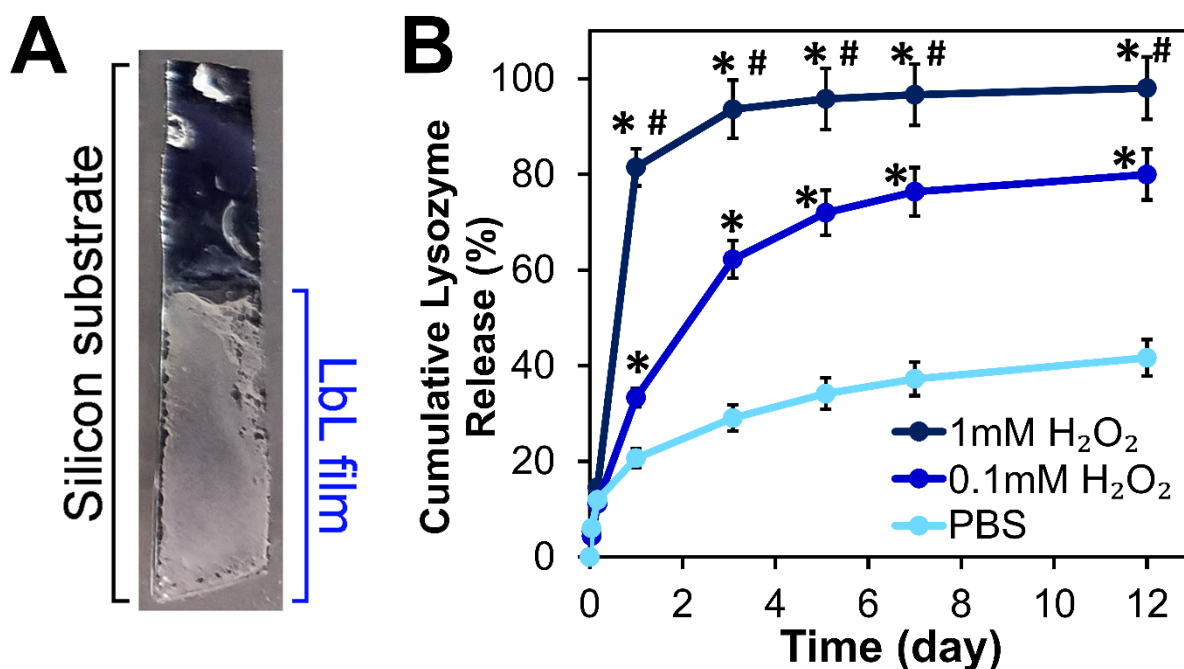


Figure S3. *In vitro* PEM films constructed with the ROS-degradable PTK-BAA polycation on (A) silicon substrates with the model protein lysozyme and 450 kDa PA. When incubated in escalating doses of H₂O₂, (B) lysozyme is increasingly released from the film indicating ROS dose-dependent drug delivery (*p<0.05 compared to PBS, #p<0.05 compared to 0.1 mM H₂O₂).

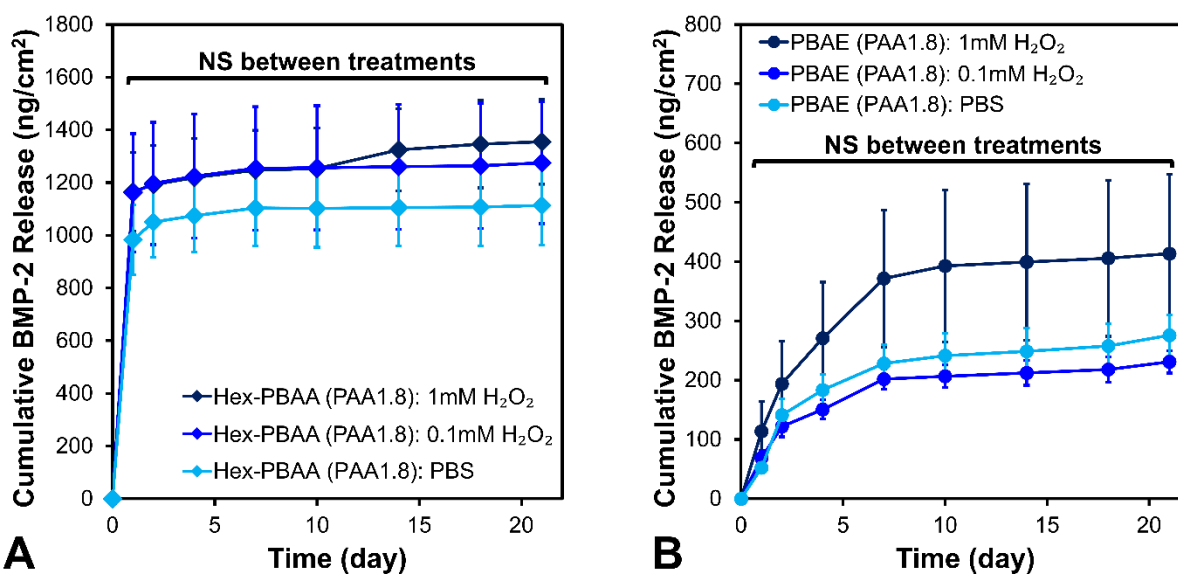


Figure S4. PEM films constructed with BMP-2, 1.8 kDa PAA, and either non-degradable hexane-PBAA or conventional PBAE polycations do not display significant differences in drug release kinetics with escalating doses of H₂O₂. All samples featured 30 tetralayer films constructed on PLGA scaffolds.

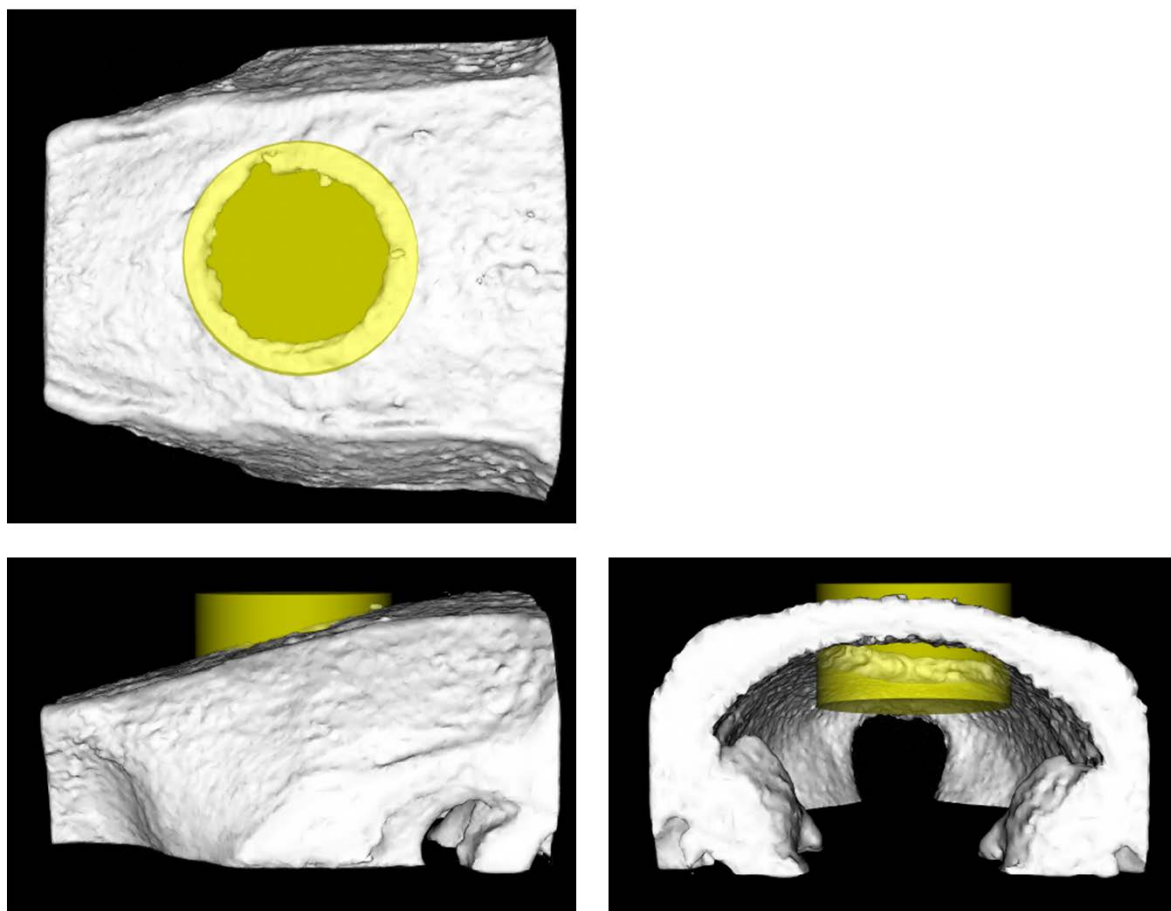


Figure S5. Representative region of interest (ROI) configuration in microcomputed tomography images of rat calvarial defects using Microview software. The 8 mm-diameter cylindrical ROI ensures that only bone growth and tissue mineralization inside the defect margins are quantified.

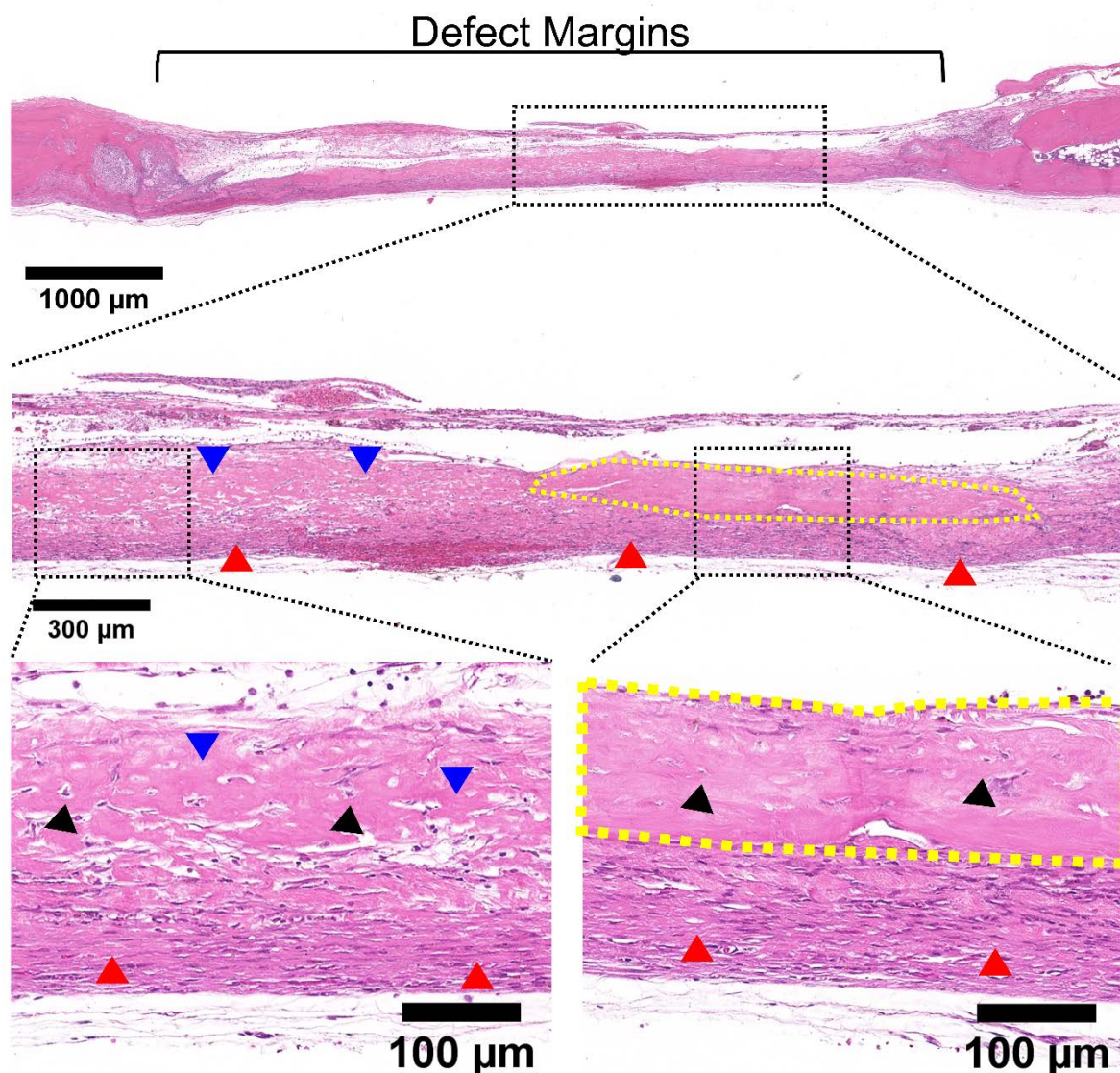


Figure S6. Histology of rat calvarial defect after 4-week treatment with a PTK-BAA / 1.8kDa PAA / BMP-2 coated PLGA scaffold. The defect does not feature full regeneration of bone tissue spanning the injury margins, but is fully bridged with a layer of fibrous tissue (red arrows) while presenting nodules of maturing bone (yellow outlines) alongside newly forming bone tissue (blue arrows). At the highest magnification, individual osteocytes are visible in the nascent bone tissue (black arrows) while highly dense regions of inflammatory immune cells or necrosis are not readily apparent.

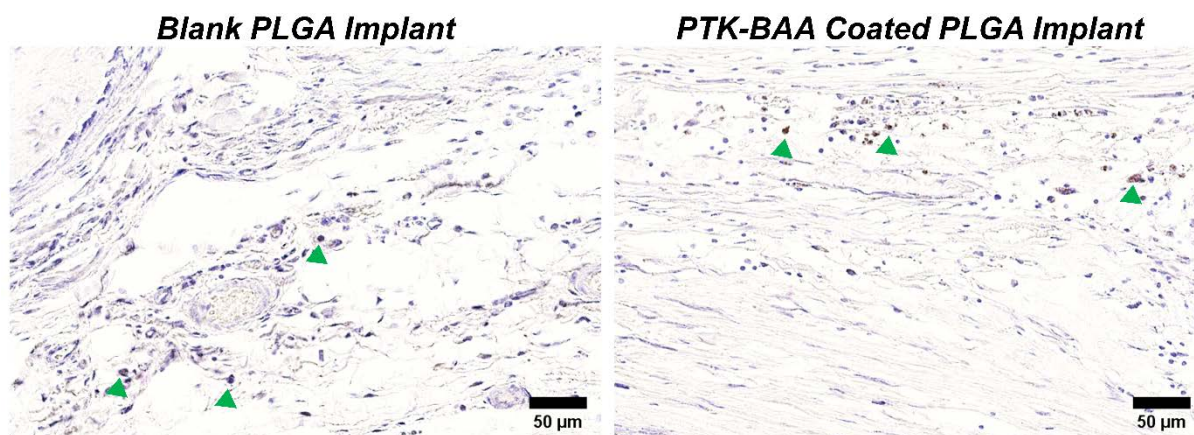


Figure S7. Immunohistochemical staining of CD68 macrophage markers in rat calvarial defects after 4-week treatment with a blank PLGA scaffold or PTK-BAA / 1.8kDa PAA / BMP-2 coated PLGA scaffold. Neither treatment group displayed an abundant macrophage presence or obvious excessive inflammatory cell manifestations, though some few macrophages were present in the healing tissues (green arrows).

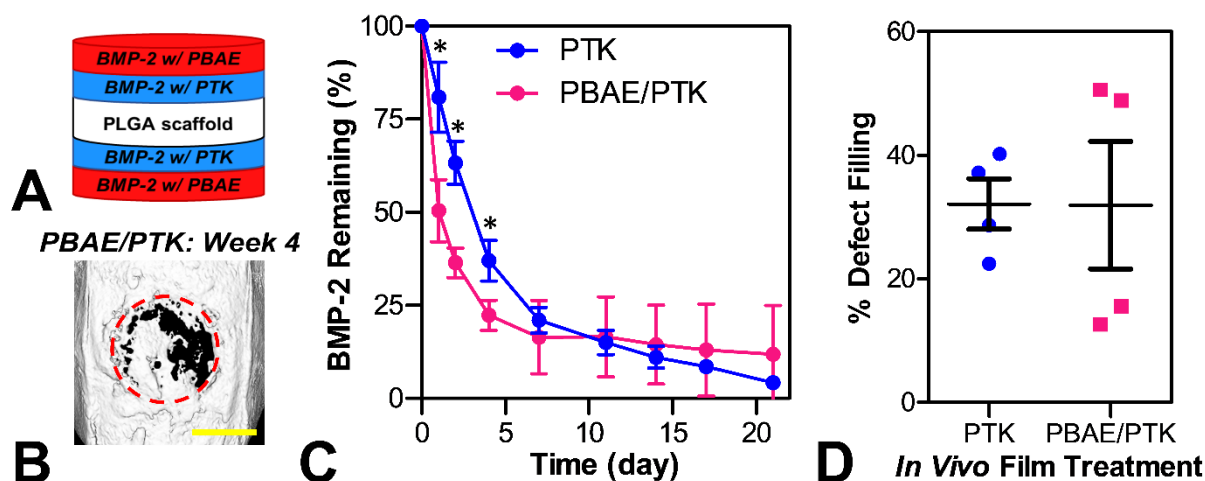


Figure S8. (A) PLGA scaffolds were coated with combination PBAE₁₅/PTK₁₅ LbL films (formed with BMP-2 and 1.8 kDa PAA, 30 tetralayers total) and implanted in (B) rat calvarial defects for 4 weeks (scale bar 5 mm). (C) Initial *in vivo* drug release from the PBAE/PTK films was significantly faster than coatings only featuring PTK polymers (**p*<0.05, *n*=3 per treatment), leading to (D) increased bone growth in some treated animals though not a statistically significant increase across the entire treatment cohort (*n*=4 per treatment).